ELSEVIER

Journal of Nuclear Materials 300 (2002) 1–6

journal of nuclear materials

www.elsevier.com/locate/jnucmat

Diffusive transport parameters and surface rate constants of deuterium in Incoloy 800

G.A. Esteban [a,*], A. Perujo [b], L.A. Sedano [c], F. Legarda [a], B. Mancinelli [b], K. Douglas [b]

[a] *Department of Nuclear Engineering and Fluid Mechanics/E.T.S.I.I.T., UPV-EHU, 48013 Bilbao, Spain*
[b] *Joint Research Centre-Ispra Site, Environment Institute, 21020 Ispra (VA), Italy*
[c] *CIEMAT, Dpt. Impacto Ambiental de la Energía, 28040 Madrid, Spain*

Received 11 July 2001; accepted 20 October 2001

Abstract

A gas permeation technique has been used to obtain the complete set of deuterium transport parameters in Incoloy 800 with deuterium driving pressures ranging from 10^4 to 1.5×10^5 Pa and temperatures from 427 to 780 K. The deuterium diffusive transport parameters obtained are: $D\ (\mathrm{m^2\,s^{-1}}) = 3.87 \times 10^{-7} \exp(-47.8\ (\mathrm{kJ\,mol^{-1}})/RT)$, $K_s\ (\mathrm{mol\,m^{-3}\,Pa^{-1/2}}) = 0.102 \exp(-7.8\ (\mathrm{kJ\,mol^{-1}})/RT)$, $\Phi\ (\mathrm{mol\,m^{-1}\,s^{-1}\,Pa^{-1/2}}) = 3.94 \times 10^{-8} \exp(-55.6\ (\mathrm{kJ\,mol^{-1}})/RT)$. The deuterium surface rate constants for a non-oxidized surface has been evaluated as: $\sigma k_1\ (\mathrm{mol\,m^{-2}\,s^{-1}\,Pa^{-1}}) = 2.67 \times 10^{-10} \exp(-40.1\ (\mathrm{kJ\,mol^{-1}})/RT)$, $\sigma k_2\ (\mathrm{mol^{-1}\,m^4\,s^{-1}}) = 2.58 \times 10^{-8} \exp(-24.5\ (\mathrm{kJ\,mol^{-1}})/RT)$, and for an oxidized surface: $(\sigma k_1)'\ (\mathrm{mol\,m^{-2}\,s^{-1}\,Pa^{-1}}) = 4.14 \times 10^{-6} \exp(-44.3\ (\mathrm{kJ\,mol^{-1}})/RT)$, $(\sigma k_2)'\ (\mathrm{mol^{-1}\,m^4\,s^{-1}}) = 4.00 \times 10^{-4} \exp(-28.6\ (\mathrm{kJ\,mol^{-1}})/RT)$.

1. Introduction

The FeNiCr alloy Incoloy 800 is increasingly being used as a steam generating (SG) material of nuclear power reactors. Its high strength and corrosion resistance properties in the presence of high-temperature water or steam make this alloy a suitable candidate material to construct the steam generator of future thermonuclear fusion reactors. Thereby, Incoloy 800 is expected to be employed in the reactor design option of the European Helium-Cooled Pebble Bed (HCPB) Blanket [1].

Some important issues to be defined when analysing the feasibility of a particular option of the reactor design are the tritium economy and the radiological safety. In relation with these matters, the evaluation of the tritium inventory absorbed within structures and released to non-radiologically protected zones is mandatory. One of the main paths for tritium release to the environment is the following: first, the helium coolant circuit receives tritium that permeates either from the first wall (FW) or the breeding zone (the last one having minor importance with respect to the FW, 0.78–8.5 g/d [1]); then, tritium is carried by the helium to the steam generator where tritium is able to be absorbed in and diffuse through the heat exchanger walls, and be carried by the steam to the thermodynamic cycle. Thereby, tritium may reach non-radiologically protected zones of the power plant.

The amount of tritium that is acceptable to be released to the environment during usual operation is about 20 Ci/day. A permeation reduction factor (PRF) of 20 in the heat exchanger walls has been evaluated to accomplish the previous condition [1]. Additionally, high PRF values will reduce the amount of hydrogen needed in the tritium recovery columns of the fuel cycle

* Corresponding author. Tel.: +34-94 601 4272; fax: +34-94 601 4159.
E-mail address: inpesalg@bi.ehu.es (G.A. Esteban).

0022-3115/02/$ - see front matter
PII: S0022-3115(01)00715-2

and, consequently, diminish the size and operational costs of that system. As a result, this high-temperature material Incoloy 800 needs a detailed analysis in relation with the hydrogen (H) isotope transport characteristics. Several works [2–8] have been carried out in order to characterize tritium permeation through Incoloy 800 together with other high-temperature SG alloys and study the inhibition of this effect by the growth of oxide layers on its surface, i.e. the use of oxide layers as effective permeation barriers.

In the present work besides permeability Φ, the diffusive deuterium transport parameters of diffusivity D and Sieverts' constant K_s have been evaluated in the temperature range 427–664 K. These parameters allow the evaluation of transient kinetics in gas transport through the diffusivity D and the total capacity of gas absorption by means of Sieverts' constant K_s, in the absence of oxide or in the presence of thermal transients that provoke stresses and induce cracks and other imperfections in the oxide film of the heat exchanger walls [8].

Alternatively, if the H transport regime becomes surface-limited [9–12] (i.e. H transport within the material is limited by the physico-chemical reactions of adsorption and recombination occurring at the surface of the material rather than the interstitial diffusion) the surface reaction rate constants of adsorption σk_1 and recombination σk_2 are the fundamental transport parameters describing the gas–material interaction. Here, σk_1 and σk_2 are evaluated in Incoloy 800 either for bare or oxidized surfaces in the temperature range 427–780 K.

2. Experimental and modelling

The material studied is the high-temperature SG FeNiCr alloy Incoloy 800, its nominal chemical composition being shown in Table 1. Clean Incoloy 800 is highly susceptible to oxidation, the characteristic of such oxide being dependent on the initial conditions of the material and its chemical and thermal exposure. The most probable oxides to be expected under oxidizing conditions are the chromium oxide Cr_2O_3 and the $MnCr_2O_4$ spinel (that have been identified as the responsible of the gas permeation inhibition [7,8]); the presence of Mn in the spinel oxide is explained by its higher diffusivity through Cr_2O_3 as compared to Cr [13].

In the present experiment, the specimen consisted of a clean polished disc of 0.4 mm thickness and 48 mm diameter. Some technological problems arose when studying bulk diffusion and absorption because of the surface oxidation. Due to the high oxidation susceptibility of Incoloy 800, in several occasions the sample had to be extracted and cleaned or be changed to eliminate the presence of oxide. Oxide growth and the corresponding gas permeation reduction could not be prevented at temperatures higher than 664 K.

When measuring the surface effects, the oxidation of the specimen at high temperature was allowed to proceed to a final stable situation where the steady-state permeation rate did not change as the time passed. After the permeation tests, the specimen was analysed by means of secondary neutral mass spectroscopy (SNMS); an oxide layer about 100 nm with an enrichment of Mn, Cr and O in the first 30 nm was detected on the surface directly exposed to deuterium gas. The surface exposed to vacuum did not show any noticeable oxide presence. The deuterium gas used was of 99.7% purity with a maximum H_2O content lower than 15 ppm.

The permeation rig and the models used to derive the transport parameters from the experimental permeation curves have been described in earlier works [14–19]. The diffusion-limited model and non-symmetric surface-limited model (Table 2) have been applied to obtain the whole set of transport parameters of Incoloy 800, including the differentiated surface-rate constant for bare and oxidized states of the material.

In this work, two consecutive methods have been applied to derive the transport constants. The first one performs a linear least-squares fitting to the steady-state permeation region with a linear equation, deriving an approximation of the transport parameters from the value of the slope S and time lag τ_L (Table 2). The second method carries out a non-linear least-squares fitting with the general expression of the fitting curve (Table 2) in both the steady-state region and the transitory region. This second fitting routine uses the transport parameters of the first step as initial values, which accelerates considerably the fitting convergence. All the values that have been obtained at different temperatures are subsequently fitted to their respective Arrhenius equations.

3. Results and discussion

In order to study the influence of oxidation on the transport regime, a group of permeation tests with different driving pressures have been performed before and after oxidation of the specimen. The measured steady

Table 1
Chemical composition (wt%) of Incoloy 800

Element	Ni	Cr	Mn	Ti	Si	Al	C	S	Fe
(wt%)	30.8	20.5	0.64	0.56	0.46	0.36	0.065	0.004	Balance

Table 2
Fitting model description: Φ—permeability, D—diffusivity, K_s—Sieverts' constant, (σk_1), $(\sigma k_1)'$—adsorption constant at high and low pressure side, respectively, R—ideal gas constant, T_{eff}—effective temperature, V_{eff}— effective volume, p_h—driving pressure, d—thickness, A—surface area, t—time

Model	Fitting law $p(t)$	Slope S	Time lag τ_L
Diffusion-limited	$p(t) = \frac{RT_{eff}}{V_{eff}}\left[\frac{\Phi p_h^{1/2}}{d}At - \frac{\Phi p_h^{1/2} d}{6D}A - \frac{2\Phi p_h^{1/2}\mathrm{d}}{6D}A \times \sum_{n=1}^{\infty}\frac{(-1)^n}{n^2}\exp(-D\frac{n^2\pi^2}{d^2}t)\right]$	$(RT_{eff}\Phi p_h^{1/2})/(V_{eff}d)$	$(d^2/6D)$
Non-symmetric surface-limited	$\frac{RT_{eff}A}{V_{eff}}(\sigma k_1)'\frac{(\sigma k_1)p_h}{(\sigma k_1)+(\sigma k_1)'}\left[t - \frac{\mathrm{d}K_s}{\sqrt{(\sigma k_1)p_h[(\sigma k_1)-(\sigma k_1)']}}\cdot \times \tanh\left(\frac{\sqrt{(\sigma k_1)p_h[(\sigma k_1)-(\sigma k_1)']}}{\mathrm{d}K_s}t\right)\right]$	$\frac{RT_{eff}A}{V_{eff}}\frac{(\sigma k_1)'(\sigma k_1)p_h}{(\sigma k_1)+(\sigma k_1)'}$	$\frac{\mathrm{d}K_s}{\sqrt{(\sigma k_1)p_h[(\sigma k_1)-(\sigma k_1)']}}$

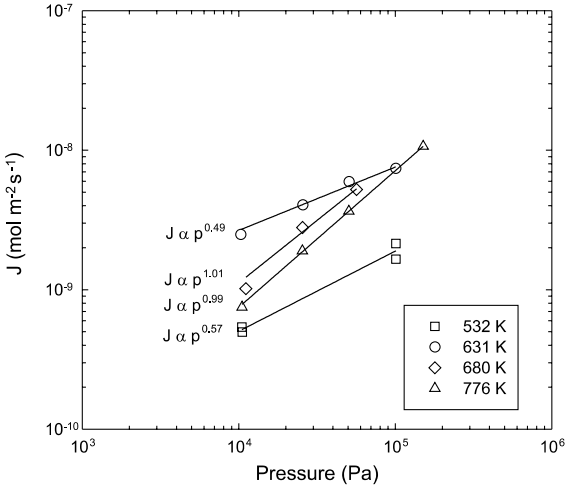

Fig. 1. Experimental deuterium permeation fluxes in Incoloy 800, dependence on driving pressure (type of transport regime).

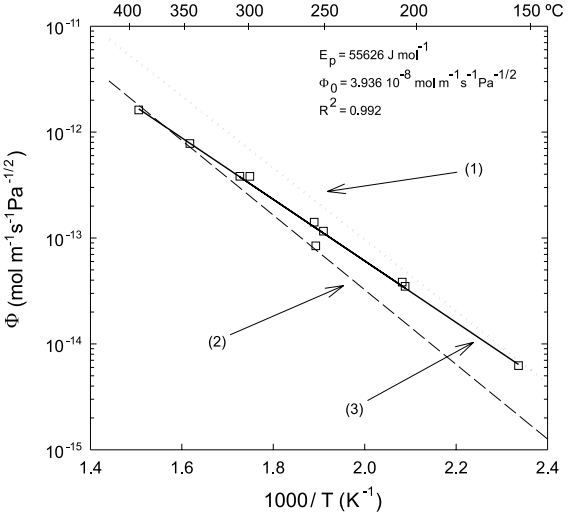

Fig. 2. Arrhenius plot of the fitted deuterium permeability in Incoloy 800: (1) hydrogen [4], (2) hydrogen (extrapolated from experimental high temperatures (923–1223 K) [5], (3) deuterium (this work).

state permeation fluxes J are depicted versus the gas driving pressures p_h for different experimental temperatures in Fig. 1; it can be noticed how the oxidation process provokes an abrupt change in the transport regime between 631 and 680 K. The pressure dependence of fluxes close to a 0.5 power relationship (characteristic of a pure diffusive transport regime) becomes a 1 power (characteristic of a pure surface limited transport regime) after oxidation. This experimental verification permits one to consider pure surface and diffusion limited transport regimes and uses the corresponding models rather than an intermediate transport regime [14].

The diffusive transport parameters have been obtained from a series of permeation tests performed in the temperature range from 427 to 664 K and driving pressures ranging from 10^4 to 1.5×10^5 Pa avoiding the influence of any surface effect. The permeability has been evaluated as (Fig. 2)

$$\Phi\ (\mathrm{mol\,m^{-1}\,s^{-1}\,Pa^{-1/2}}) = 3.94 \times 10^{-8} \times \exp(-55.6\ (\mathrm{kJ\,mol^{-1}})/RT), \quad (1)$$

the diffusivity (Fig. 3)

$$D\ (\mathrm{m^2\,s^{-1}}) = 3.87 \times 10^{-7}\exp(-47.8\ (\mathrm{kJ\,mol^{-1}})/RT), \quad (2)$$

and Sieverts' constant (Fig. 4)

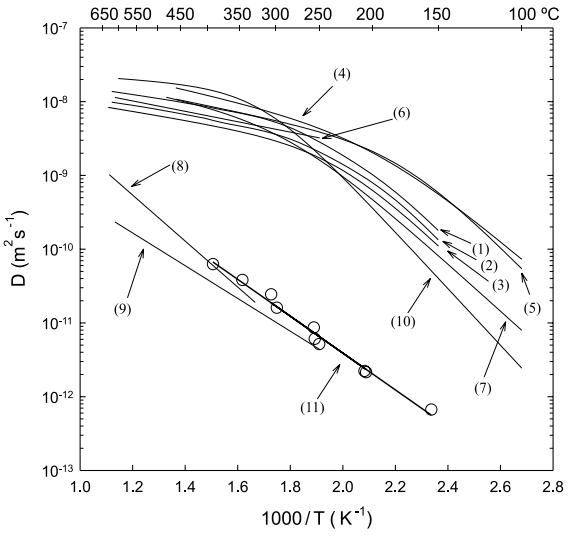

Fig. 3. Diffusivity in Incoloy 800 compared with reference steels: (1), (2) and (3) H_2, D_2 and T_2, respectively, in OPTIFER-IVb [22], (4) D_2 in Batman [19], (5) D_2 in F82H [19], (6) H_2 in MANET [16], (7) H_2 in MANET [20], (8) H_2 in SS 316L [20], (9) H_2 in SS 316L [21], (10) H_2 in α-Fe [23], (11) D_2 in Incoloy 800 (this work).

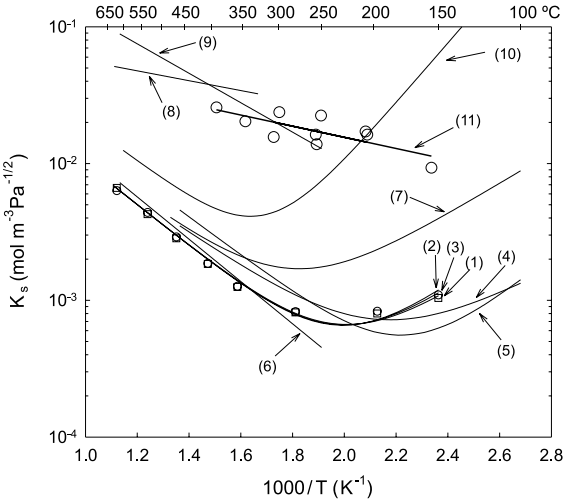

Fig. 4. Sieverts' constant in Incoloy 800 compared with reference steels: (1), (2) and (3) H_2, D_2 and T_2, respectively, in OPTIFER-IVb [22], (4) D_2 in Batman [19], (5) D_2 in F82H [19], (6) H_2 in MANET [16], (7) H_2 in MANET [20], (8) H_2 in SS 316L [20], (9) H_2 in SS 316L [21], (10) H_2 in α-Fe [23], (11) D_2 in Incoloy 800 (this work).

$$K_s\ (\mathrm{mol\,m^{-3}\,Pa^{-1/2}}) = 0.102\ \exp(-7.8\ (\mathrm{kJ\,mol^{-1}})/RT). \tag{3}$$

In Fig. 2, it can be noticed how the present result of permeability approximates well to those obtained by Bell et al. [4] and Schaefer et al. [5]. To the knowledge of the authors K_s and D of any hydrogen isotope have not been independently studied in Incoloy 800 hitherto. No trapping effect on diffusivity and Sieverts' constant has been noticed throughout the whole experimental temperature range; the pronounced increase of K_s and decrease of D at temperatures approximately below 573 K detected in ferritic–martensitic steels [22] have not been observed here. It can be noticed how well Incoloy 800 matches the results of austenitic stainless steel rather than the results of the ferritic–martensitic ones. This fact confirms the relationship between the chemical composition of the alloys and the hydrogen isotope transport parameters [24], because Incoloy 800 approximates better the high Ni and Cr contents of austenitic stainless steel than the ferritic–martensitic one. Furthermore, the diffusion activation energy of deuterium in Incoloy 800 ($E_d = 47.8$ kJ mol^{-1}) is analogous to the high values detected for the austenitic stainless steel AISI 316L ($E_d = 42.5$ kJ mol^{-1} [20] or 59.7 kJ mol^{-1} [21]), differing from the typical low values of the ferritic–martensitic ones (all the referenced steels of this type show $E_d < 16.0$ kJ mol^{-1} [19,22,23]).

The surface transport parameters have been obtained from a series of permeation tests performed in the temperature range from 427 to 780 K and driving pressures ranging from 10^4 to 1.5×10^5 Pa, once the growth of the oxide layer on the surface facing the high-pressure atmosphere had stabilized. For the oxidized surface (high-pressure region) the adsorption constant has been evaluated as (Fig. 5)

$$\sigma k_1\ (\mathrm{mol\,m^{-2}\,s^{-1}\,Pa^{-1}}) = 2.67 \times 10^{-10} \times \exp(-40.1\ (\mathrm{kJ\,mol^{-1}})/RT) \tag{4}$$

and the recombination constant (Fig. 6)

$$\sigma k_2\ (\mathrm{mol^{-1}\,m^4\,s^{-1}}) = 2.58 \times 10^{-8}\ \exp(-24.5\ (\mathrm{kJ\,mol^{-1}})/RT). \tag{5}$$

For the non-oxidized surface (low-pressure region) the adsorption constant has been evaluated as (Fig. 5)

$$(\sigma k_1)'(\mathrm{mol\,m^{-2}\,s^{-1}\,Pa^{-1}}) = 4.14 \times 10^{-6} \times \exp(-44.3\ (\mathrm{kJ\,mol^{-1}})/RT) \tag{6}$$

and the recombination constant (Fig. 6)

$$(\sigma k_2)'(\mathrm{mol^{-1}\,m^4\,s^{-1}}) = 4.00 \times 10^{-4} \times \exp(-28.6\ (\mathrm{kJ\,mol^{-1}})/RT). \tag{7}$$

The resulting surface rate constants for the high-pressure region (oxide present) are more than three

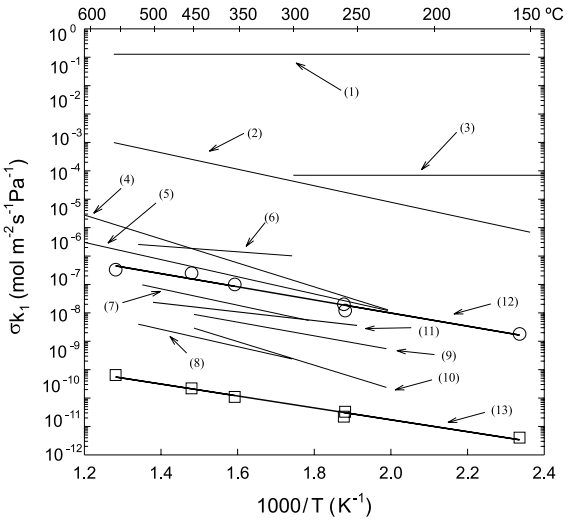

Fig. 5. Arrhenius plot of adsorption rate constants: (1) and (2) Pick and Sonnenberg model [11] and Baskes model [10], respectively, for Incoloy 800 (with sticking coefficient $s = 1$ and roughness $\sigma = 1$), (3) D^+ implantation in MANET [25], (4) H_2 in 316 SS ion beam cleaned [26], (5) H_2 in 316 SS oxidized both surfaces [26], (6) D_2 in bare MANET [15], (7) D_2 in MANET [18], (8) D_2 in oxidized MANET [15], (9) D_2 in Inconel 600 [27], (10) D_2 in 304 SS [28], (11) D_2 in bare OPTIFER-IVb [14], (12) D_2 in bare Incoloy 800 (this work), (13) D_2 in oxidized Incoloy 800 (this work).

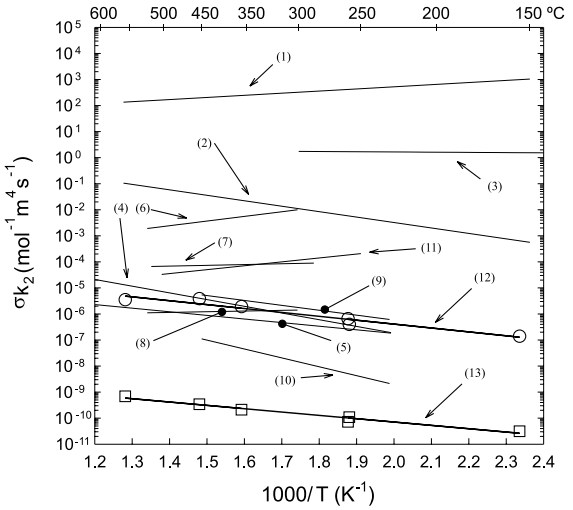

Fig. 6. Arrhenius plot of recombination rate constants: (1) and (2) Pick and Sonnenberg [11] model and Baskes [10] model, respectively, for Incoloy 800 (with sticking coefficient $s = 1$ and roughness $\sigma = 1$), (3) D^+ implantation in MANET [25], (4) H_2 in 316 SS ion beam cleaned [26], (5) H_2 in 316 SS oxidized both surfaces [26], (6) D_2 in bare MANET [15], (7) D_2 in MANET [18], (8) D_2 in oxidized MANET [15], (9) D_2 in Inconel 600 [27], (10) D_2 in 304 SS [28], (11) D_2 in bare OPTIFER-IVb [14], (12) D_2 in bare Incoloy 800 (this work), (13) D_2 in oxidized Incoloy 800 (this work).

orders of magnitude lower than the resulting surface rate constants for the low-pressure region (oxide absent). Furthermore, the values for $(\sigma k_1)'$ and $(\sigma k_2)'$ that have been obtained for the oxidized surfaces of Incoloy 800 are the lowest in comparison to the steels. It is worth noting that the recombination constant of Incoloy 800 shows a positive activation energy, as it is the general behaviour of the austenitic stainless steels, in opposition to the ferritic–martensitic ones. This fact may be the consequence of similar characteristics of the oxide produced in the high-Cr-content alloys. These features show the great influence of the oxide on the surface parameters entailing the inhibition of the hydrogen isotope transport and confirms the possibility of 'in situ' generating effective permeation barriers with an oxide layer on Incoloy 800 whenever the oxide stability is assured. The permeation rate reduction derived here, $(J_{\text{bare}}/J_{\text{oxide}}) > 10^3$, is even higher than those obtained by means of the classic aluminide coatings (optionally oxidized as Al_2O_3) used as permeation barriers [29,30].

The Baskes [10] and Pick and Sonnenberg [11] models, on the basis of kinetic statistics, provide analytical expressions for the surface-rate constants. The Baskes model for Incoloy 800 yields an activation energy of adsorption 55.6 kJ mol^{-1} comparable to the experimental 40.1 and 44.3 kJ mol^{-1}; the existing gap between the experimental and theoretical values (Figs. 5 and 6) may be attributed to sticking coefficients of 5.26×10^{-10} and 8.17×10^{-6} corresponding to oxidized and non-oxidized surfaces, respectively. The Pick and Sonnenberg model denotes a major mismatch because the model foresees no activation energy for adsorption when the experimental results accounted for it. The model could be congruent with the experimental values provided the sticking coefficient was activated with the energies of 40.1 and 44.3 kJ mol^{-1} for oxidized and non-oxidized surfaces, respectively.

4. Conclusions

The gas permeation technique has been used to investigate deuterium transport in Incoloy 800. Two well-differentiated transport regimes have been discriminated: a diffusion-limited and a surface-limited regime, both of them have been individually simulated with their respective theoretical model. Satisfactory diffusive transport parameters D, K_s and Φ have been obtained in the temperature range 427–664 K.

The surface rate constants of adsorption σk_1 and recombination σk_2 have been evaluated in the temperature range 427–780 K. The state of each surface of the specimen has been differentiated by means of a non-symmetric model. A gap close to four orders of magnitude between the surface rate constants evaluated in the presence and in the absence of oxide has been evidenced.

The layer of the spinel oxide $MnCr_2O_4$ has demonstrated to be an effective hydrogen isotope transport barrier.

Acknowledgements

The authors would like to thank Mr G.B. Cueroni for the valuable technical support offered in the setting up and the maintenance of the hydrogen permeation facility.

References

[1] L. Berardinucci, M.D. Donne, Proceedings of the SOFT, Lisbon, Fus. Technol. 2 (1996) 1427.
[2] A. Perujo, J. Reimann, H. Feuerstein, B. Mancinelli, J. Nucl. Mater. 283–287 (2000) 1292.
[3] M.A. Fütterer, X. Raepsaet, E. Proust, Fus. Eng. Des. 29 (1995) 225.
[4] J.T. Bell, J.D. Redman, H.F. Bittner, Metall. Trans. 11A (1980) 775.
[5] J. Schaefer, D. Stöver, R. Hecker, Nucl. Technol. 66 (1984) 537.
[6] H.P. Buchkremer, R. Hecker, H. Jonas, D. Stöver, U. Zink, Nucl. Technol. 66 (1984) 550.
[7] R.A. Strehlow, H.C. Savage, J. Nucl. Mater. 53 (1974) 323.
[8] R.A. Strehlow, H.C. Savage, Nucl. Technol. 22 (1974) 127.
[9] P.M. Richards, J. Nucl. Mater. 152 (1988) 246.
[10] M.I. Baskes, J. Nucl. Mater. 92 (1980) 318.
[11] M.A. Pick, K. Sonnenberg, J. Nucl. Mater. 131 (1985) 208.
[12] A.D. Le Claire, in: The Permeation of Gases Through Solids. I—Principles, UKAEA Harwell, AERE-R 9911, 1981.
[13] R.K. Wild, Corros. Sci. 17 (1977) 87.
[14] G.A. Esteban, A. Perujo, L.A. Sedano, B. Mancinelli, J. Nucl. Mater. 282 (2000) 89.
[15] E. Serra, A. Perujo, J. Nucl. Mater. 240 (1997) 215.
[16] E. Serra, A. Perujo, K.S. Forcey, Vuoto 3 (1997) 18.
[17] A. Perujo, K. Douglas, E. Serra, Fus. Eng. Des. 31 (1995) 101.
[18] E. Serra, A. Perujo, J. Nucl. Mater. 223 (1995) 157.
[19] E. Serra, A. Perujo, G. Benamati, J. Nucl. Mater. 245 (1997) 108.
[20] K.S. Forcey, D.K. Ross, J.C.B. Simpson, J. Nucl. Mater. 160 (1988) 117.
[21] F. Reiter, J. Camposilvan, M. Caorlin, G. Saibene, R. Sartori, Fus. Technol. 8 (1985) 2344.
[22] G.A. Esteban, A. Perujo, K. Douglas, L.A. Sedano, J. Nucl. Mater. 281 (2000) 34.
[23] K.S. Forcey, I. Iordanova, M. Yaneva, J. Nucl. Mater. 240 (1997) 118.
[24] P. Jung, J. Nucl. Mater. 238 (1996) 189.
[25] L.A. Sedano, A. Perujo, J. Camposilvan, G.B. Cueroni, K. Douglas, in: The deuterium recombination and dissociation constants in MANET derived from plasma implantation experiments, JRC–Ispra, EUR 17713 EN, 1997.
[26] D.M. Grant, D.L. Cummings, D.A. Blackburn, J. Nucl. Mater. 152 (1988) 139.
[27] E. Rota, F. Waelbroeck, P. Wienhold, J. Winter, J. Nucl. Mater. 111&112 (1982) 233.
[28] M. Braun, B. Emmoth, F. Waelbroeck, P. Wienhold, J. Nucl. Mater. 93&94 (1980) 861.
[29] A. Perujo, K.S. Forcey, T. Sample, J. Nucl. Mater. 207 (1993) 86.
[30] K.S. Forcey, D.K. Ross, C.H. Wu, J. Nucl. Mater. 182 (1991) 36.